Journal of Materials Chemistry

Cite this: J. Mater. Chem., 2012, 22, 23439

www.rsc.org/materials

PAPER

Benzoxazole and benzimidazole heterocycle-grafted graphene for high-performance supercapacitor electrodes†

Wei Ai,[ab] Weiwei Zhou,[b] Zhuzhu Du,[a] Yaping Du,[c] Hua Zhang,[c] Xingtao Jia,[b] Linghai Xie,*[a] Mingdong Yi,[a] Ting Yu*[b] and Wei Huang*[a]

Received 6th August 2012, Accepted 14th September 2012
DOI: 10.1039/c2jm35234f

An efficient method for the preparation of benzoxazole and benzimidazole covalently grafted graphene and their application as high performance electrode materials for supercapacitors is reported. The synthesis of such covalently functionalized graphene materials first involves a cyclization reaction of carboxylic groups on graphene oxide with the hydroxyl and aminos groups on *o*-aminophenol and *o*-phenylenediamine, and subsequent reduction by hydrazine. Results of Fourier transformed infrared spectroscopy (FT-IR), Raman spectroscopy, X-ray photoelectron spectroscopy (XPS), X-ray diffraction (XRD) and thermogravimetric analysis (TGA) have confirmed that the covalent functionalization of graphene is achieved through the formation of benzoxazole and benzimidazole on the graphene sheets. The functionalized graphene materials are revealed to consist of corrugation and scrolling morphologies with less aggregation, indicating the effectiveness of functionalization in preventing restacking/aggregation of the graphene sheets. Furthermore, when applied as supercapacitor electrodes, the functionalized graphene materials exhibit good electrochemical performances in terms of high specific capacitance (730 and 781 F g^{-1} for benzoxazole and benzimidazole grafted graphene, respectively, at a current density of 0.1 A g^{-1}) and good cycling stability, implying their potential for energy storage applications.

1. Introduction

Development of advanced functional materials for energy conversion and storage technologies is crucial in addressing the challenges of global warming and the finite nature of fossil fuels.[1] Supercapacitors, also known as ultracapacitors, which store energy based on either ion adsorption (electrochemical double layer capacitor, EDLCs) or fast/reversible faradaic reactions (pseudocapacitors) have attracted intensive attention, mainly due to their high power density, long cycle life and low maintenance requirements, as well as their safety.[2] However, the widespread use of supercapacitors is limited by their low energy density and relatively high effective series resistance. As a consequence, it is clear that the development of various strategies and techniques for fabricating supercapacitors with high specific capacitance and high power density is needed to meet the demand for high-performance devices.[3]

Graphene, a rapidly rising star on the horizon of materials science, has been widely explored in energy-related areas, including organic photovoltaic cells, lithium ion batteries and as a support for fuel cell catalysts, because of its fascinating physical and chemical properties.[4–6] The high conductivity, low mass density, high mechanical strength, and large specific surface area of graphene and its derivatives also make them attractive as electrode materials for supercapacitors.[7–9] It is expected that graphene with less agglomeration would exhibit higher effective surface area, and thus better capacitive performance.[10] In this regard, graphene oxide (GO) resulting from solution exfoliation of graphite is considered to be an exciting precursor for low-cost and mass production of graphene-based materials with single or few layer sheets. Unfortunately, the GO sheets tend to either form irreversible agglomerates or restack during the solution reduction process, leading to loss of the surface area for supercapacitor applications.[11,12] Many feasible active species, such as conducting polymers and transition metal oxides, have been introduced to prevent the restacking of graphene sheets, as well as to improve the performance of graphene-based supercapacitor

[a]*Key Laboratory for Organic Electronics & Information Displays (KLOEID) and Institute of Advanced Materials (IAM), Nanjing University of Posts and Telecommunications, 9 Wenyuan Road, Nanjing 210046, P. R. China. E-mail: iamlhxie@njupt.edu.cn; wei-huang@njupt.edu.cn; Fax: +86 25 8349 2333; Tel: +86 25 8349 2333*
[b]*Division of Physics and Applied Physics, School of Physical and Mathematical Sciences, Nanyang Technological University, 637371, Singapore. E-mail: yuting@ntu.edu.sg; Fax: +65 63167899; Tel: +65 63167899*
[c]*School of Materials Science and Engineering, Nanyang Technological University, 639798, Singapore*

† Electronic supplementary information (ESI) available: Raman spectroscopy, XPS spectra and the element content data of GO, BO-G and BI-G. See DOI: 10.1039/c2jm35234f

electrodes, due to their contribution of additional redox capacitance.[13,14] However, the composites usually suffer from rapid fading of capacity, due to the volume change and ion dissolution during charge–discharge processes.[15,16] Covalent functionalization of GO followed by reduction has also proved to be an effective way of tuning the chemical and electrical structure of graphene for supercapacitors.[17] Additionally, functionalized graphene-based materials are expected to exhibit better supercapacitor performances due to the introduction of redox-active functional groups, which can enhance the charge storage capability by providing fast redox processes at the electrode surface.[18,19]

Based on these considerations, in this work we report an efficient method for the synthesis of covalently functionalized graphene materials, with less aggregation and abundant redox-active azole functional groups, and their application as electrode materials for supercapacitors. Typically, GO was first treated with *o*-aminophenol (OAP) or *o*-phenylenediamine (OPD) in the presence of polyphosphoric acid (PPA) as a catalyst. Subsequent reduction of the functionalized GO by hydrazine results in the benzoxazole or benzimidazole heterocycle grafted graphene materials. The introduction of benzoxazole and benzimidazole onto the graphene sheets could inhibit the aggregation of graphene sheets and consequently form a stable 3D conducting network. These structural and morphological advantages result in higher specific capacitance (730 F g^{-1} for benzoxazole-grafted graphene and 781 F g^{-1} for benzimidazole-grafted graphene, respectively) compared with previously reported graphene materials at the same current density, as well as good stability when the as-prepared materials are used as supercapacitor electrode materials in an aqueous electrolyte.[20,21] This newly developed strategy provides a good example of the application of covalently functionalized graphene in high-performance energy-storage devices.

2. Experimental section

2.1 Materials

Graphite powder (<20 μm), sulfuric acid (H_2SO_4), potassium permanganate ($KMnO_4$), hydrogen peroxide (H_2O_2), PPA, OAP, OPD and hydrochloric acid (HCl) were purchased from Sigma-Aldrich Pte Ltd and used without further purification.

2.2 Synthesis of GO

GO was synthesized from graphite (Aldrich; <20 μm) by a modified Hummers' method.[22] Graphite powder (1.0 g) was added into 50 mL of concentrated H_2SO_4 (95%) under stirring in an ice bath, and then $KMnO_4$ (6 g) was slowly added to the suspension to keep the reaction temperature lower than 20 °C. The ice bath was then removed and the mixture was stirred at 30 °C for 1 hour. Subsequently, deionized water (80 mL) was slowly added under vigorous stirring. The diluted suspension was further stirred at 90 °C for 30 min. Afterwards, deionized water (200 mL) with 30% H_2O_2 (6 mL) was added, turning the color of the solution from dark brown to yellow. The suspension was stirred for additional 10 min, then centrifugated and washed with deionized water several times, and finally freeze-dried in a freeze drying machine.

2.3 Synthesis of benzoxazole and benzimidazole-grafted graphene

The syntheses of benzoxazole and benzimidazole covalently functionalized graphene *via* a PPA-catalyzed cyclization reaction followed by reduction with hydrazine are shown in Scheme 1. Firstly, GO solution (2 mg mL^{-1}) was prepared by ultrasonic exfoliation of graphite oxide (160 mg) into deionized water (80 mL) for 30 min. OAP–OPD (700 mg) was added into the solution and sonicated for another 5 min. After that PPA (1 mL) was added dropwise under vigorous stirring, and the solution was refluxed at 80 °C in darkness for 24 hours. The product was collected by filtration, re-dissolved in 1 : 2 HCl by sonication and then collected by filtration (this procedure was repeated 4 times). After washing with deionized water several times, the obtained product was redispersed into methanol (120 mL) by sonication for 30 min, then hydrazine hydrate (1.4 mL) was added and refluxed at 65 °C for 24 hours. The obtained benzoxazole and benzimidazole-grafted graphene, abbreviated as BO-G and BI-G, respectively, were filtered and washed with methanol several times, then dried under vacuum condition for 24 hours.

2.4 Characterization

FT-IR spectra were recorded on a NEXUS 670 FT-IR spectrometer by using pressed KBr pellets. XPS analysis was performed on an ESCALAB MK II X-ray photoelectron spectrometer. Field-emission scanning electron microscopy (FESEM) analysis was conducted with a JEOL JSM-6700F electron microscope with an accelerating voltage of 10 kV. Transmission electron microscopy (TEM) measurements were conducted on a JEOL JEM-2010 transmission electron microscope with an accelerating voltage of 200 kV. XRD analysis was measured on a D8 Advanced diffractometer with Cu-K radiation ($\lambda = 1.54056$ Å). Raman spectra were collected using a WITEC CRM200 Raman system with 532 nm excitation laser. TGA was conducted by a Shimadzu DTG-60H under a heating rate of 5 °C min^{-1} under nitrogen flow.

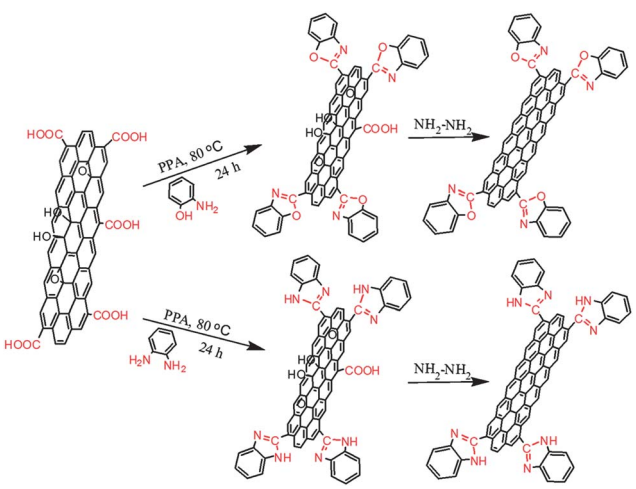

Scheme 1 Synthesis procedure for benzoxazole and benzimidazole-grafted graphene *via* heterocyclization reaction.

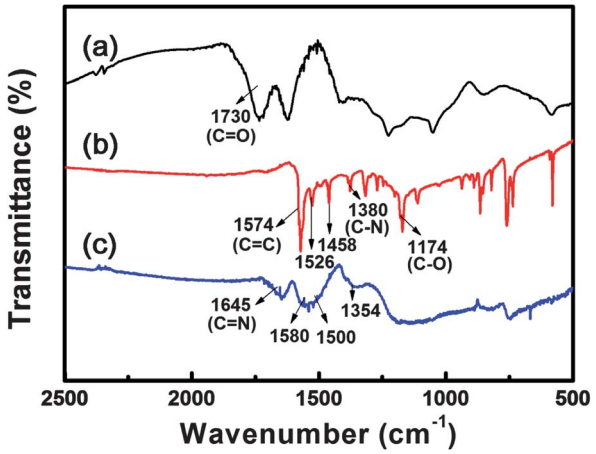

Fig. 1 FT-IR spectra of GO (a), BO-G (b) and BI-G (c).

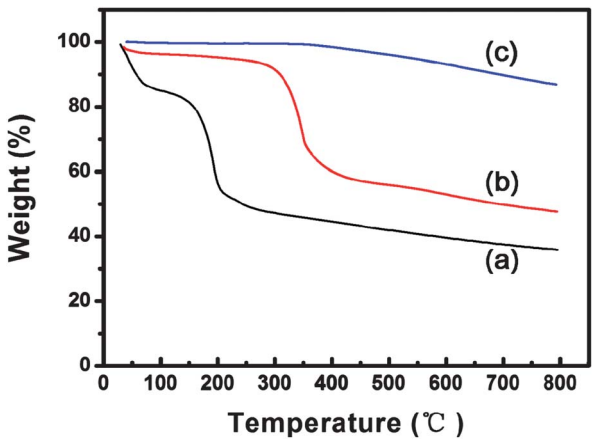

Fig. 2 Thermogravimetric curves of GO (a), BO-G (b) and BI-G (c) at heating rate 5 °C min^{-1} under nitrogen atmosphere.

2.5 Electrochemical measurements

A three-electrode cell system was used to evaluate the electrochemical performance of the functionalized graphene materials on a CHI 760D electrochemistry workstation with 1 mol L^{-1} H_2SO_4 aqueous solution as the electrolyte. The working electrode was prepared by casting a Nafion-impregnated sample onto a glassy carbon electrode with diameter of 5 mm.[23] Typically, 5 mg of active material was dispersed in 1 mL of ethanol solution containing 5 μL of Nafion solution (5 wt% in water) by sonication for 30 min to form a catalyst ink. 20 μL of the as-prepared ink was then dropped onto the glassy carbon electrode and baked at 80 °C for 10 min before the electrochemical test. Platinum foil (1 cm × 1 cm) and a Ag/AgCl electrode were used as the counter and reference electrodes, respectively. Cyclic voltammetry (CV) studies were performed with a potential window from −0.3 to 0.7 V for benzoxazole-grafted graphene and −0.5 to 0.5 V for benzimidazole-grafted graphene at scan rates of 100, 50, 20, 10 and 5 mV s^{-1}. The specific capacitance (SC) is calculated by using the integrated area of the CV curve to obtain the charge (Q), and dividing by the mass of the active material (m) and the scanning rate (V):

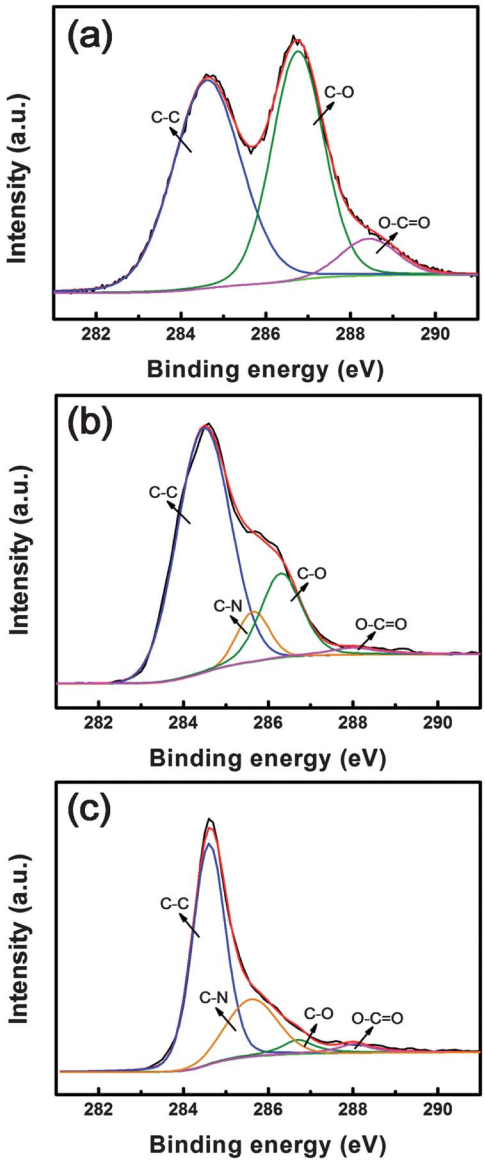

Fig. 3 The C 1s XPS spectra of GO (a), BO-G (b) and BI-G (c).

$$C = Q/2mV$$

Galvanostatic charge–discharge curves were measured at different constant current densities. The SC can also be calculated using galvanostatic charge–discharge curves by the following equation:

$$C = I\Delta t/m\Delta V$$

Where m is also the mass of electrode material, ΔV is the potential window, I is the discharge current applied and Δt is the discharge time.

3. Results and discussion

3.1 Materials characterization

The FT-IR spectra of GO, BO-G and BI-G materials are shown in Fig. 1. The most characteristic adsorption band of GO at 1730 cm^{-1} corresponds to the C=O stretching mode of carboxyl

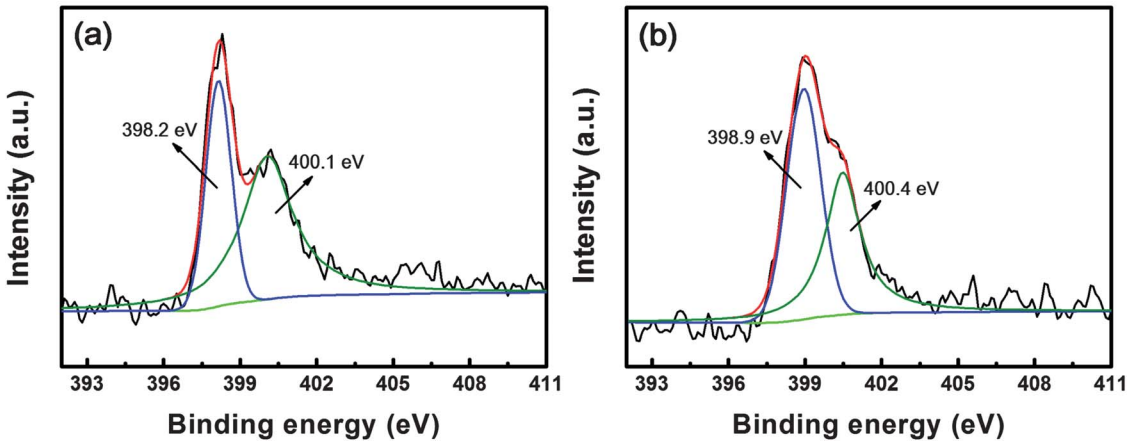

Fig. 4 The N 1s XPS spectra of BO-G (a) and BI-G (b).

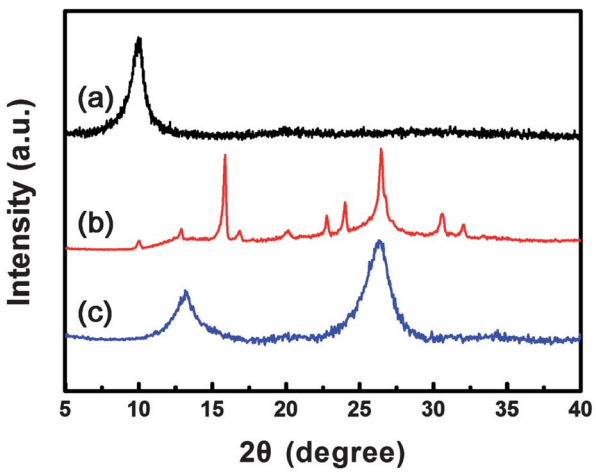

Fig. 5 XRD patterns of GO (a), BO-G (b) and BI-G (c).

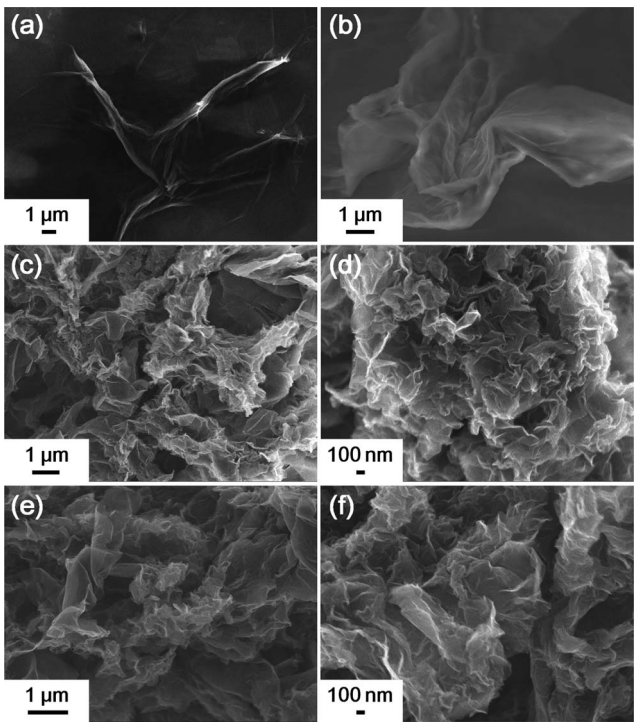

Fig. 6 FESEM images of the GO (a and b), BO-G (c and d) and BI-G (e and f) powder.

groups on the GO sheets. However, after functionalization and reduction, the peak at 1730 cm^{-1} disappeared. In the spectrum of BO-G, the new peaks at 1574, 1526 and 1458 cm^{-1} are attributed to the skeletal vibration modes of the benzene ring.[24] The other two peaks at 1380 and 1174 cm^{-1} can be assigned to the stretching mode of C–N and C–O from benzoxazole heterocycle, respectively.[25] In the spectrum of BI-G, the skeletal vibration modes of the benzene ring appear at 1580 and 1500 cm^{-1}. However, another two typical peaks at 1645 cm^{-1} and 1354 cm^{-1} are also observed, which can be attributed to the stretching mode of C=N and C–N from benzimidazole heterocycle, respectively.[26] Raman spectroscopy was also used to confirm the presence of benzoxazole and benzimidazole heterocycle grafted onto the graphene sheets (Fig. S1†). The Raman bands of oxazole and imidazole heterocycles can be clearly observed in the Raman spectra of BO-G and BI-G, which is consistent with previous results.[27,28]

TGA thermogram also clearly supports the cyclization reaction of graphene, as shown in Fig. 2. GO shows ~15% mass loss near 100 °C due to the removal of adsorbed water molecules trapped between the sheets (Fig. 2a).[29] A relatively large loss of mass in the range of 150–260 °C is also observed, which is ascribed to the decomposition of the labile oxygen-contained groups in GO-based materials.[30] However, compared to GO, both the benzoxazole and benzimidazole grafted graphene show a significantly smaller mass loss around 100 °C owing to the removal of oxygen-containing functional groups (Fig. 2b and c). The thermogram of BO-G illustrates a major mass loss in the range of 290–410 °C, which is attributed to the decomposition of benzoxazole groups covalently grafted on the graphene sheets.[31] The BI-G thermogram has one significant mass loss starting at about 400 °C, due to the decomposition of benzimidazole groups.[32] The TGA results indicate the successful functionalization of graphene, resulting in a higher thermal stability.

The covalent grafting of benzoxazole and benzimidazole onto the graphene sheets *via* the cyclization reaction was further

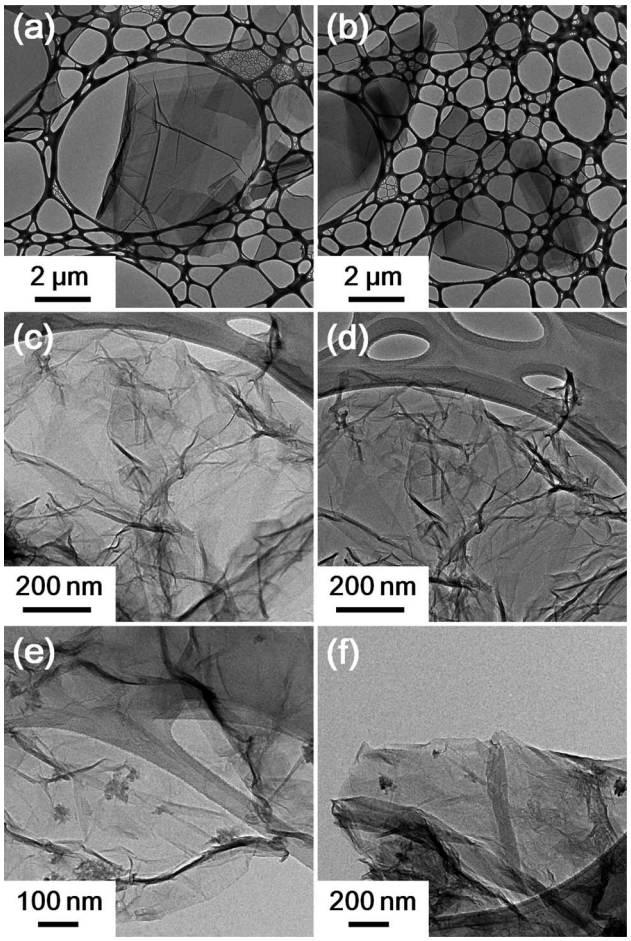

Fig. 7 TEM images of the GO (a and b), BO-G (c and d) and BI-G (e and f).

confirmed by XPS. The C 1s XPS spectra of original GO (Fig. 3a) consists of three peaks arising from C–C (284.6 eV), C–O (286.7) and O–C=O (288.4 eV). After the functionalization and reduction, the peak intensity for oxygen-containing groups decreased remarkably, while the peak of the sp^2 carbon increased significantly (Fig. 3b and c and S2†). These results indicate that most of the oxygen functional groups in GO have been successfully removed after reduction. Furthermore, an additional type of carbon at about 285.6 eV is observed, which originates from C–N.[33] The obvious N 1s peaks at 399 eV in the XPS spectra of BO-G and BI-G also confirm the existence of nitrogen-containing groups on these two functionalized graphene (Fig. S2†), while no N 1s signal is detected in GO. The total atomic ratios in the samples, calculated from quantitative analysis of the XPS data, are shown in Table S1.†

The bonding configurations of N atoms in BO-G and BI-G were further investigated by high-resolution N 1s XPS spectra (Fig. 4). The N 1s peaks of both BO-G and BI-G could be fitted as two peaks, a higher energy peak at about 400.1 eV and a lower energy peak at about 398.2 eV, which correspond to pyridine-like N and the pyrrole-like N from the introduced heterocyclic groups, respectively.[34] The N 1s peak of BO-G at 398.2 eV is generated from the aromatic nitrogen doping during the reduction, which is consistent with previous reports.[35]

Fig. 5 shows the XRD patterns of GO, BO-G and BI-G. The characteristic diffraction peak of GO appears at 9.98°, corresponding to an interlayer distance of 8.85 Å due to the intercalation of oxygen-containing functional groups on the graphite sheets (Fig. 5a).[36] In accordance with previous analyses, after the functionalization and reduction most of the oxygen-containing groups are removed. Both the XRD patterns of BO-G and BI-G exhibit two main peaks. One is in the angle range of $2\theta = 13$–$16°$, which is due to the presence of benzoxazole and benzimidazole groups on the graphene sheets resulting in an increased interlayer distance between the sheets. The other (at 26.3°) is representative of chemically converted graphene (CCG),[37] indicating the restacking of some unfunctionalized areas on the surface of the graphene sheets. The XRD results indicate that the introduction of benzoxazole and benzimidazole groups can partially prevent the restacking of graphene sheets.

FESEM and TEM were also used to characterize GO, BO-G and BI-G. The results are shown in Fig. 6 and 7. The synthesized GO shows a typically crumpled morphology, a layer-like structure with a lateral dimension up to several micrometers (Fig. 6a and b and 7a and b), which is consistent with previous reports in the literature.[38] Fig. 6c–f present the SEM images of BO-G and BI-G, revealing that the layered structure can be maintained in the functionalized graphene after the treatments. Moreover, less aggregation was observed, indicating the effectiveness of functionalization for the prevention of restacking/aggregation of graphene sheets, supporting the above XRD results (Fig. 5).

The TEM images in Fig. 7c–f reveal that the BO-G and BI-G materials consist of randomly aggregated, thin, crumpled sheets, interconnected with each other, resembling rippled silk waves. This structure may favorably improve the electrochemical performance of the functionalized graphene, as the corrugation and scrolling dominate the functionalized graphene sheet, forming a three-dimensional (3D) conducting network for fast electron transfer between the active materials and the charge collector.[39]

3.2 Electrochemical measurements

To explore the advantages of BO-G and BI-G as electrode materials for supercapacitors, their electrochemical properties were analyzed by standard CV and galvanostatic charge–discharge techniques. Fig. 8a and b show the CV curves of BO-G and BI-G, respectively, at scan rates of 5–100 mV s^{-1}. For BO-G material, two oxidation peaks at −0.09 (A_1) and 0.27 V (A_2) are observed in the anodic process and three reduction peaks at −0.24 (C_1), −0.14 (C_2), and 0.15 V (C_3) are observed in the cathodic process.

The oxidation peak A_1 and reduction peaks C_1 and C_2 may correspond to the electrochemical reaction of the remaining oxygen-containing functional groups on the functionalized graphene sheets (Scheme 2, eqn (1) and (2)).[40] The second redox couple A_2/C_2 is probably related to the faradaic reaction of benzoxazole units grafted on graphene sheets at the electrode/electrolyte interfaces (Scheme 2, eqn (3)).[41,42] While for BI-G material, a couple of redox peaks at −0.23 (C'_1) and −0.04 V (A'_1) are observed, resulting from the introduced benzimidazole groups (Scheme 2, eqn (4)).[43]

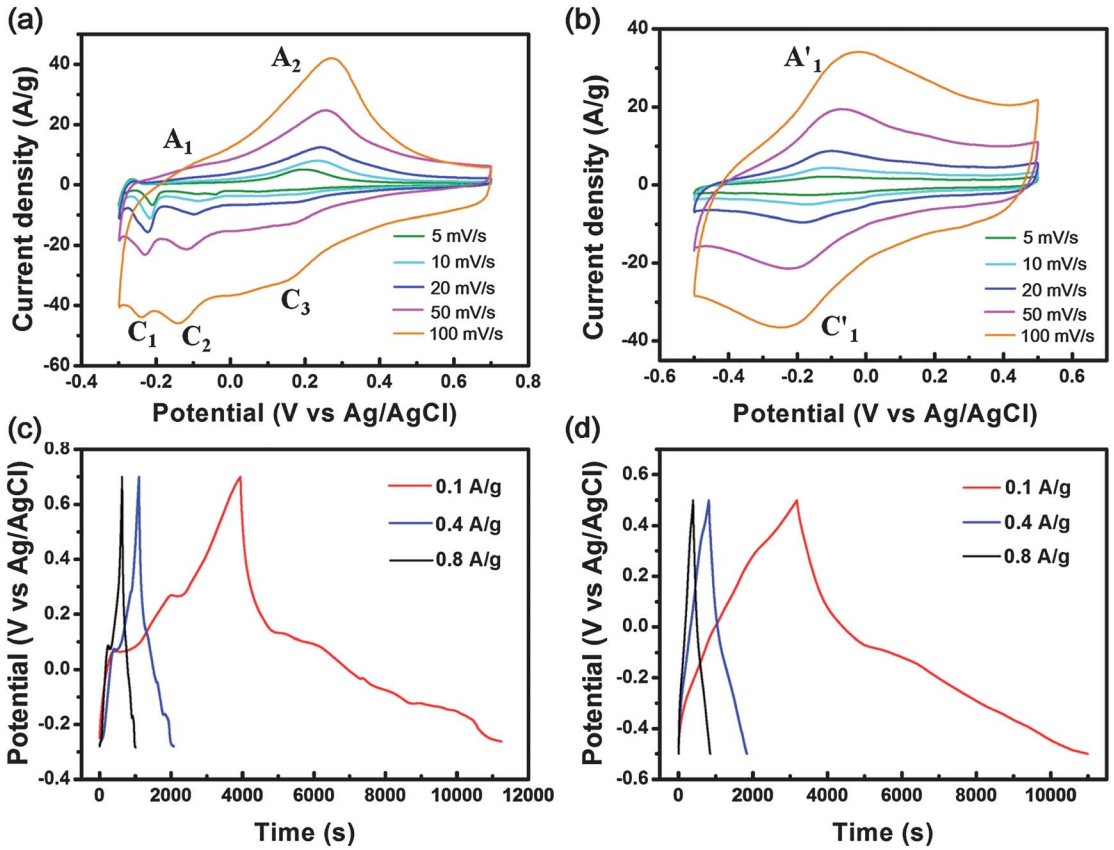

Fig. 8 CVs for the BO-G (a) and BI-G (b) materials at different scan rates; charge–discharge curves of BO-G (c) and BI-G (d) at different galvanostatic current densities.

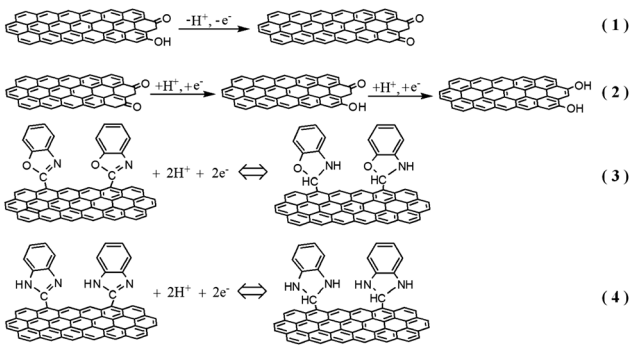

Scheme 2 The proposed electrochemical reactions of redox-active functional groups on BO-G and BI-G.

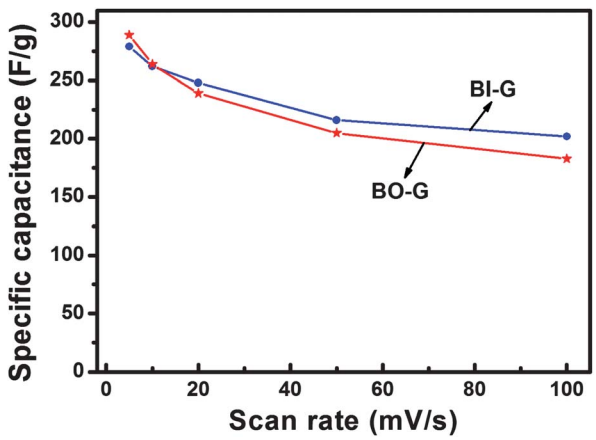

Fig. 9 SC of BO-G and BI-G materials measured as a function of scan rate.

The capacitance values of BO-G and BI-G, calculated from CV curves, are shown in Fig. 9. The largest SCs for BO-G and BI-G are 289 and 279 F g^{-1}, respectively, which can both be reached at a scan rate of 5 mV s^{-1}. The observed phenomenon of increasing SCs with decreasing scan rate is due to the decreasing diffusion limitation.[44]

The electrochemical performances of BO-G and BI-G materials were further studied by galvanostatic charge–discharge measurement. Fig. 8c and d show the charge–discharge curves of BO-G and BI-G at different current densities. The nonlinear potential profiles were measured, indicating the contribution of pseudocapacitance due to the faradaic reaction.[45] The SCs of BO-G derived from the discharging curves are 730 F g^{-1} at 0.1 A g^{-1}, 391 F g^{-1} at 0.4 A g^{-1}, and 296 F g^{-1} at 0.8 A g^{-1}. For BI-G material, the SCs are 781 F g^{-1}, 410 F g^{-1}, and 367 F g^{-1} at current densities of 0.1 A g^{-1}, 0.4 A g^{-1}, and 0.8 A g^{-1}, respectively. These values are much higher than those of CCG,[20,21,46] demonstrating the feasibility of improving the SC of graphene materials by introducing oxazole or imidazole groups.

Cycling stability is one of the most important parameters for supercapacitors. The BO-G and BI-G materials were tested for

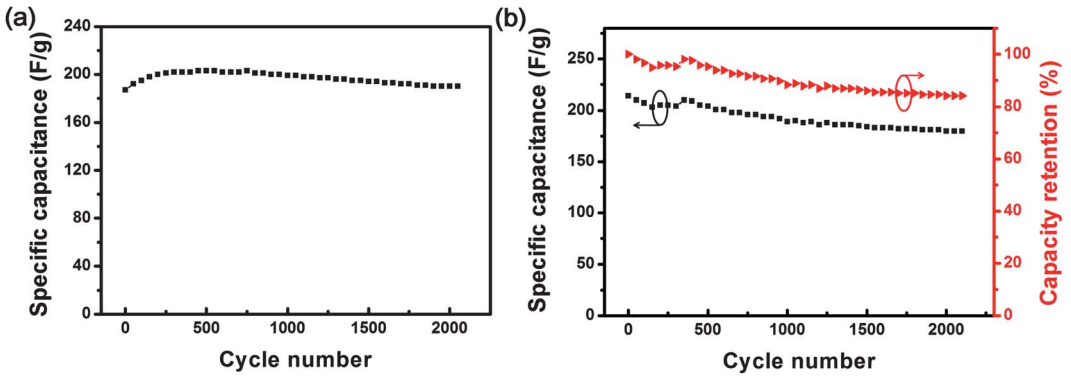

Fig. 10 Cycle performance of BO-G (a) and BI-G (b) materials measured at a scan rate of 100 mV s^{-1}.

2000 cycles at a scan rate of 100 mV s^{-1}. The results reveal that both BO-G and BI-G materials show quite good cycling stability (Fig. 10). Specifically, the BO-G material exhibits a stable electrochemical performance with no obvious SC drop after 2000 cycles (Fig. 10a). The initial increase of SC during the first 500 cycles is possibly due to the activation process, which allows the trapped ions to gradually diffuse out.[7,39] Moreover, the BI-G material also presents an excellent long-term stability with 85% of the original capacitance retained after 2000 cycles (Fig. 10b). The good electrochemical performance of the BO-G and BI-G materials can be ascribed to their unique, well-packed, layered structure, which not only provide easy access of the surfaces to electrolyte but also prevents the agglomeration of graphene sheets.

4. Conclusions

In summary, we have demonstrated an efficient method to prepare benzoxazole and benzimidazole covalently grafted graphene. The structure, surface morphology and electrochemical behaviors of the functionalized graphene are thoroughly investigated. The incorporation of benzoxazole and benzimidazole functional groups on graphene can prevent the restacking of graphene sheets, and also improve the electrode/electrolyte interfacial charge transfer process. Thus, high specific capacitance and good cycling stability can be ensured. Further improvements in tuning the microstructure of the functionalized graphene sheets, and hence their electrochemical properties, are in progress.

Acknowledgements

This work was supported by the "973" project (no. 2009CB930600, 2012CB933301), NNSFC (grants no. 21144004, 61136003, 51173081, 20974046, 50428303), The Program for New Century Excellent Talents in University (NCET-11-0992), the Ministry of Education of China (no. IRT1148), the NSF of Jiangsu Province (grants no. SBK201122680, 11KJB510017, BK2008053, 11KJB510017, BZ2010043 and no. BK2009025) and NUPT (no. NY210030 and NY211022). The authors acknowledge Dr Taixing Tan from Key Laboratory of Functional Inorganic Material Chemistry (Heilongjiang University), Ministry of Education for help with the TGA characterization, Dr Huanping Yang (School of Physical and Mathematical Sciences, Nanyang Technological University) and Dr Jilei Liu (School of Physical and Mathematical Sciences, Nanyang Technological University) for their useful discussions.

Notes and references

1 A. S. Arico, P. Bruce, B. Scrosati, J. M. Tarascon and W. van Schalkwijk, *Nat. Mater.*, 2005, **4**, 366.
2 Y. Huang, J. Liang and Y. Chen, *Small*, 2012, **12**, 1805.
3 J. Jiang, J. Liu, W. Zhou, J. Zhu, X. Huang, X. Qi, H. Zhang and T. Yu, *Energy Environ. Sci.*, 2011, **4**, 5000.
4 C. X. Guo, H. B. Yang, Z. M. Sheng, Z. S. Lu, Q. L. Song and C. M. Li, *Angew. Chem., Int. Ed.*, 2010, **49**, 3014.
5 W. W. Zhou, J. X. Zhu, C. W. Cheng, J. P. Liu, H. P. Yang, C. X. Cong, C. Guan, X. T. Jia, H. J. Fan, Q. Y. Yan, C. M. Li and T. Yu, *Energy Environ. Sci.*, 2011, **4**, 4954.
6 X. Xie, G. Yu, N. Liu, Z. Bao, C. S. Criddle and Y. Cui, *Energy Environ. Sci.*, 2012, **5**, 6862.
7 X. Cao, Y. Shi, W. Shi, G. Lu, X. Huang, Q. Yan, Q. Zhang and H. Zhang, *Small*, 2011, **7**, 3163.
8 Y. W. Zhu, S. Murali, M. D. Stoller, K. J. Ganesh, W. W. Cai, P. J. Ferreira, A. Pirkle, R. M. Wallace, K. A. Cychosz, M. Thommes, D. Su, E. A. Stach and R. S. Ruoff, *Science*, 2011, **332**, 1537.
9 M. F. El-Kady, V. Strong, S. Dubin and R. B. Kaner, *Science*, 2012, **335**, 1326.
10 M. D. Stoller, S. Park, Y. Zhu, J. An and R. S. Ruoff, *Nano Lett.*, 2008, **8**, 3498.
11 D. Yu and L. Dai, *J. Phys. Chem. Lett.*, 2009, **1**, 467.
12 S. Bai and X. Shen, *RSC Adv.*, 2012, **2**, 64.
13 W. Chen, S. Li, C. Chen and L. Yan, *Adv. Mater.*, 2011, **23**, 5679.
14 G. Zhou, D. W. Wang, F. Li, L. Zhang, N. Li, Z.-S. Wu, L. Wen, G. Q. Lu and H. M. Cheng, *Chem. Mater.*, 2010, **22**, 5306.
15 N. A. Kumar, H. J. Choi, A. Bund, J. B. Baek and Y. T. Jeong, *J. Mater. Chem.*, 2012, **22**, 12268.
16 L. Mao, K. Zhang, H. S. On Chan and J. Wu, *J. Mater. Chem.*, 2012, **22**, 1845.
17 Q. Wu, Y. Sun, H. Bai and G. Shi, *Phys. Chem. Chem. Phys.*, 2011, **13**, 11193.
18 B. Xu, S. Yue, Z. Sui, X. Zhang, S. Hou, G. Cao and Y. Yang, *Energy Environ. Sci.*, 2011, **4**, 2826.
19 C. X. Guo and C. M. Li, *Energy Environ. Sci.*, 2011, **4**, 4504.
20 K. Zhang, L. L. Zhang, X. S. Zhao and J. Wu, *Chem. Mater.*, 2010, **22**, 1392.
21 K. Zhang, L. Mao, L. L. Zhang, H. S. On Chan, X. S. Zhao and J. Wu, *J. Mater. Chem.*, 2011, **21**, 7302.
22 X. Jiang, Y. W. Ma, J. J. Li, Q. L. Fan and W. Huang, *J. Phys. Chem. C*, 2010, **114**, 22462.
23 W. Zhou, J. Liu, T. Chen, K. S. Tan, X. Jia, Z. Luo, C. Cong, H. Yang, C. M. Li and T. Yu, *Phys. Chem. Chem. Phys.*, 2011, **13**, 14462.
24 U. Kortz, M. G. Savelieff, F. Y. A. Ghali, L. M. Khalil, S. A. Maalouf and D. I. Sinno, *Angew. Chem., Int. Ed.*, 2002, **41**, 4070.
25 H. Reyes, H. I. Beltran and E. Rivera-Becerril, *Tetrahedron Lett.*, 2011, **52**, 308.

26 H. Leutbecher, M. A. Constantin, S. Mika, J. Conrad and U. Beifuss, *Tetrahedron Lett.*, 2011, **52**, 605.
27 M. Muniz-Miranda, *Vib. Spectrosc.*, 1999, **19**, 227.
28 L. M. Markham, L. C. Mayne, B. S. Hudson and M. Z. Zgierski, *J. Phys. Chem.*, 1993, **97**, 10319.
29 V. H. Pham, T. V. Cuong, S. H. Hur, E. Oh, E. J. Kim, E. W. Shin and J. S. Chung, *J. Mater. Chem.*, 2011, **21**, 3371.
30 S. H. Lee, D. R. Dreyer, J. An, A. Velamakanni, R. D. Piner, S. Park, Y. Zhu, S. O. Kim, C. W. Bielawski and R. S. Ruoff, *Macromol. Rapid Commun.*, 2010, **31**, 281.
31 J. H. Kim and J. K. Lee, *Bull. Korean Chem. Soc.*, 2001, **22**, 999.
32 M. G. Rabbani and H. M. El-Kaderi, *Chem. Mater.*, 2012, **24**, 1511.
33 N. I. Kovtyukhova and T. E. Mallouk, *J. Phys. Chem. B*, 2005, **109**, 2540.
34 Y. Wang, Y. Shao, D. W. Matson, J. Li and Y. Lin, *ACS Nano*, 2010, **4**, 1790.
35 S. Park, Y. Hu, J. O. Hwang, E. S. Lee, L. B. Casabianca, W. Cai, J. R. Potts, H.-W. Ha, S. Chen, J. Oh, S. O. Kim, Y. H. Kim, Y. Ishii and R. S. Ruoff, *Nat. Commun.*, 2012, **3**, 638.
36 D. C. Marcano, D. V. Kosynkin, J. M. Berlin, A. Sinitskii, Z. Sun, A. Slesarev, L. B. Alemany, W. Lu and J. M. Tour, *ACS Nano*, 2010, **4**, 4806.
37 H. P. Yang, J. Jiang, W. W. Zhou, L. F. Lai, L. F. Xi, Y. M. Lam, Z. X. Shen, B. Khezri and T. Yu, *Nanoscale Res. Lett.*, 2011, **6**, 531.
38 A. Dimiev, D. V. Kosynkin, L. B. Alemany, P. Chaguine and J. M. Tour, *J. Am. Chem. Soc.*, 2012, **134**, 2815.
39 K. K. Lee, S. Deng, H. M. Fan, S. Mhaisalkar, H. R. Tan, E. S. Tok, K. P. Loh, W. S. Chin and C. H. Sow, *Nanoscale*, 2012, **4**, 2958.
40 K. R. Mahanthesha, B. E. K. Swamy, U. Chandra, Y. D. Bodke, K. V. K. Pai and B. S. Sherigara, *Int. J. Electrochem. Sci.*, 2009, **4**, 1237.
41 E. Frackowiak, *Phys. Chem. Chem. Phys.*, 2007, **9**, 1774.
42 E. Frackowiak and F. Beguin, *Carbon*, 2001, **39**, 937.
43 L. Lai, L. Chen, D. Zhan, L. Sun, J. Liu, S. H. Lim, C. K. Poh, Z. Shen and J. Lin, *Carbon*, 2011, **49**, 3250.
44 D. N. Futaba, K. Hata, T. Yamada, T. Hiraoka, Y. Hayamizu, Y. Kakudate, O. Tanaike, H. Hatori, M. Yumura and S. Iijima, *Nat. Mater.*, 2006, **5**, 987.
45 X. Lu, G. Wang, T. Zhai, M. Yu, J. Gan, Y. Tong and Y. Li, *Nano Lett.*, 2012, **12**, 1690.
46 L. L. Zhang, S. Zhao, X. N. Tian and X. S. Zhao, *Langmuir*, 2010, **26**, 17624.

